

On the Principles of Modelling of Homogeneous–Heterogeneous Reactions in the Production of Fine Chemicals. A Case Study: Reductive Alkylation of Aromatic Amines

Juha Lehtonen,[†] Tapio Salmi,^{*,†} Antti Vuori,[‡] and Esko Tirronen[‡]

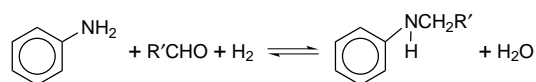
Laboratory of Industrial Chemistry, Åbo Akademi, FIN-20500, Åbo, Finland, and Research Centre, Kemira Agro Oy, FIN-02771, Espoo, Finland

Abstract:

A kinetic model for the reductive alkylation of aromatic amines, which implies a combination of homogeneous and heterogeneous reactions, was developed. The kinetic model was combined with a reactor model for a semibatch reactor, traditionally used for the reductive alkylation on both laboratory and industrial scale. The system was modelled as a three-phase system, with mass-transfer limitations at the gas–liquid interface. The mass-transfer resistances at the outer surface of the catalyst and inside the catalyst were considered to be negligible, since very finely dispersed catalyst particles were used. The kinetic parameters were determined for a system containing an aromatic amine with one alkyl substituent and an aldehyde. The results revealed that it is possible to describe this kind of complex reaction system with very few parameters.

Introduction

Reductive alkylation of substituted anilines is a widely used reaction in the production of intermediates in the dyestuff industry. The overall liquid-phase reaction, where the amino group reacts with aldehyde and hydrogen molecules, producing a secondary amine and abstracting water is presented as



The reaction route goes through hemiaminal and imine intermediates. The secondary amine is further dialkylated, and the aromatic ring can also undergo an alkylation reaction. In principle, many other side reactions take place in the system, for example, the dimerization of the aromatics as well as different reactions between the aldehydes. Besides the amino group, there may exist one or two substituents attached to the aromatic ring.

The reactions are traditionally carried out in a pressurized semibatch reactor,¹ where the first step, a noncatalytic thermal alkylation in the liquid phase, is followed by the

second step, a heterogeneously catalyzed reductive hydrogenation. For the catalytic step, platinum, palladium, and nickel catalysts are typically used. The complexity of the system is increased due to the mass-transfer effects of the three-phase system: a gas phase with hydrogen, a liquid phase with the aromatics, the aldehyde, and the solvent, and a solid catalyst are present.

In the present study, a semibatch reactor model is combined with the mass-transfer equations for the phase interfaces and the rate equations for homogeneous and heterogeneous steps. As a demonstration system, reductive alkylation of an aromatic amine with one alkyl substituent in the ortho position with a short-chain aldehyde (fewer than three carbon atoms) is used. Kinetic parameters are determined and a simplification procedure of the kinetic model is presented in this paper.

The reactor model is valid for both laboratory and industrial scale reactors. On industrial scale, loop reactors can be used for reductive alkylation in order to suppress the mass-transfer limitations at the gas–liquid interface.¹ The scale-up of the actual system to the industrial scale and the model for the loop reactor will be presented in a separate paper.

Reactions

The mechanisms of the reaction steps in the reductive alkylation are well described in the standard textbooks of organic chemistry. The reaction proceeds principally in three steps. In the first step, the amino group reacts with an aldehyde, producing an intermediate (**M1**). In the second step, the intermediate (**M1**) is decomposed to imine (Schiff's base) (**M2**) and water,² whereas the third step is a heterogeneously catalyzed hydrogenation of the imine.³ In principle, the secondary amine (**B**) can also be formed directly from the carbinolamine (**M1**) by hydrogenolysis.⁴ It is not necessary to consider these two mechanisms separately, since the kinetic equations become very similar. The reaction steps are given by eqs 1–3.

[†] Åbo Akademi.

[‡] Kemira Agro Oy.

(1) Malone, R. J.; Merten, H. L. A Comparative Mass Transfer Study in the Reductive N-Alkylation of Aromatic Nitro Compounds. *Chem. Ind.* **1992**, 47, 79–85.

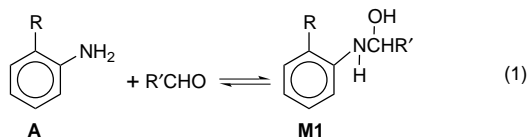
(2) Ege, S. *Organic Chemistry, Structure and Reactivity*, 3rd ed.; D. C. Heath and Comp.: Lexington, 1994; p 535.

(3) Fox, M. A.; Whitesell, J. K. *Organic Chemistry*; Jones and Bartlett Publishers: Boston, 1994; p 72.

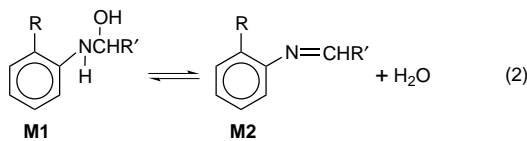
(4) Bonds, A. P.; Greenfield, H. The Reductive Alkylation of Aromatic Amines with Formaldehyde. *Chem. Ind.* **1992**, 47, 65–78.

monoalkylation of the amino group:

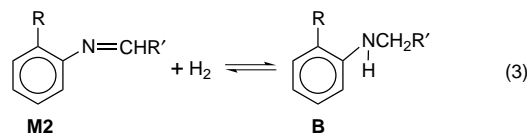
1. homogeneous reaction in the liquid phase



2. homogeneous reaction in the liquid phase



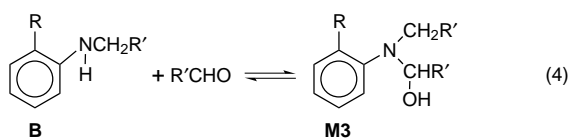
3. heterogeneous surface reaction



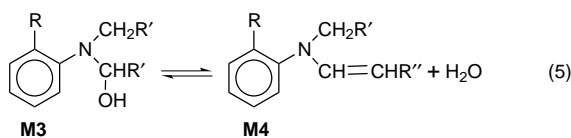
The monoalkylated compound can be dialkylated, or the aldehyde can react directly with the aromatic ring, which is alkylated. The dialkylation reaction and the alkylation of the aromatic ring may involve intermediates similar to those that appear in the monoalkylation of the amino group. The reaction steps in the dialkylation of the amino group, eqs 4–6, and in the alkylation of the aromatic ring, eqs 7–9, are summarized as follows:

dialkylation of the amino group:

1. homogeneous reaction in the liquid phase

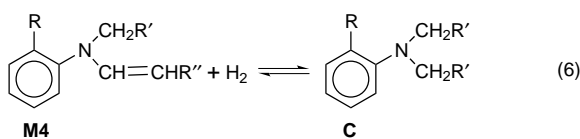


2. homogeneous reaction in the liquid phase



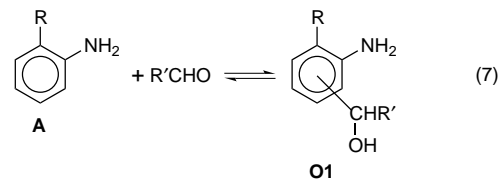
where $\text{R}'' = \text{R}' - \text{CH}_2$

3. heterogeneous surface reaction

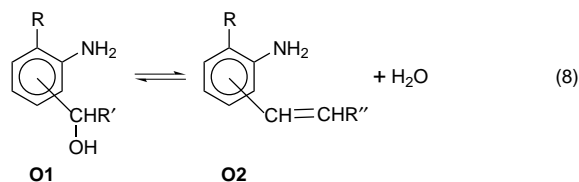


alkylation of the aromatic ring:

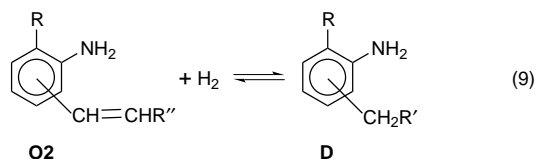
1. homogeneous reaction in the liquid phase



2. homogeneous reaction in the liquid phase



3. heterogeneous surface reaction



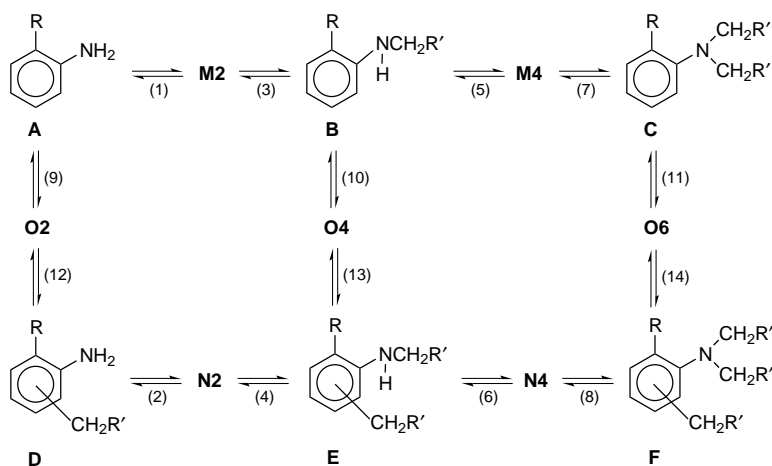
Besides the reactions presented above, several side reactions can also take place, for example, the dimerization of two aromatic rings. In this reaction, two aromatic rings react with the aldehyde, forming a dimer and abstracting water. Principally all aromatic compounds can undergo dimerization.

The side reactions of the aldehydes are typically very complex.⁴ The aldehyde may exist as a hydrate in water or as an acetal or a hemiacetal in the alcoholic solvent. Aldehyde might also undergo a catalytic hydrogenation to alcohol, or two aldehyde molecules might undergo aldol condensation. The presence of these side reactions is strongly dependent on the properties of the aldehyde and on the reaction conditions. The side reactions can be suppressed by a gradual addition of the aldehyde in order to maintain a low concentration of the aldehyde.⁴ Under our experimental conditions, the formation of the by-products listed above was very minor due to slow addition of aldehyde. Therefore only the alkylation reactions 1–9 are included in the reaction scheme (Scheme 1). According to this scheme, it is assumed that the aromatic ring of monoalkylated and dialkylated compounds can be alkylated further and the ring-alkylated compounds can undergo monoalkylation and dialkylation of the amino group.

Kinetics and Stoichiometry

Monoalkylation and dialkylation of the amino group as well as the alkylation of the aromatic ring are presumed to have analogous reaction mechanisms (eqs 1–9), which implies that a separate derivation of the kinetic equations is unnecessary. The first and second steps are considered to be homogeneous reactions in the liquid phase; the heterogeneous catalyst being present in the system has no influence

Scheme 1. Reaction scheme of reductive alkylation of aromatic amines



on these steps. The third step is assumed to be a surface process on a platinum catalyst: the aromatic compound produced in step II reacts with hydrogen on the active sites of the catalyst.

The two initiating homogeneous steps (eqs 1 and 2) can be written as



where **II** and **I2** denote intermediates in the alkylation reactions. The first step (I) is presumed to be slow (rate-determining), whereas the second one (II) is rapid. The following rate equation can thus be obtained for the step I:

$$r_1 = k_1 \left(c_A c_{\text{R}'\text{CHO}} - \frac{c_{\text{II}}}{K_1} \right) \quad (10)$$

The rapid step gives the quasi-equilibrium expression

$$K_2 = \frac{c_{\text{I2}} c_{\text{H}_2\text{O}}}{c_{\text{II}}} \quad (11)$$

which is inserted into the rate equation

$$r_1 = k_1 \left(c_A c_{\text{R}'\text{CHO}} - \frac{c_{\text{I2}} c_{\text{H}_2\text{O}}}{K_1 K_2} \right) \quad (12)$$

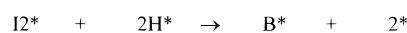
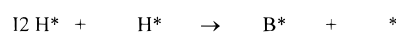
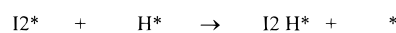
where

$$K_1 K_2 = \frac{c_{\text{I2}} c_{\text{H}_2\text{O}}}{c_A c_{\text{R}'\text{CHO}}} = K_{\text{I2}} \quad (13)$$

The reaction steps I and II have been considered as reversible in the derivation of the rate expressions. The mechanism via hydrogenolysis of carbinolamine (hemiaminal) gives a very analogous rate expression for the homogeneous steps.

The third step is a surface reaction on the Pt catalyst. The following reaction mechanism is introduced for the rate-determining surface reaction, assuming dissociative hydrogen

adsorption, consecutive hydrogen addition, and product desorption:



On the basis of this mechanism, the rate equation

$$r_3 = k_3 \Theta_{\text{I2}} \Theta_{\text{H}}^2 \quad (14)$$

is obtained, where **I2** can be **M2**, **M4**, **N2**, **N4**, **O2**, **O4**, or **O6**.

The following quasi-equilibrium approximations are used for the rapid adsorption steps:

$$K_{\text{H}} = \frac{\Theta_{\text{H}}^2}{c_{\text{H}_2} \Theta_{\text{V}}^2} \quad (15)$$

$$K_{\text{I2}} = \frac{\Theta_{\text{I2}}}{c_{\text{I2}} \Theta_{\text{V}}} \quad (16)$$

Since also other aromatic compounds, not only the reacting compound, as well as water and the solvent (alcohol), are presumably to be adsorbed on the catalyst surface, we obtain analogously

$$K_j = \frac{\Theta_j}{c_j \Theta_{\text{V}}} \quad (17)$$

where *j* denotes any adsorbed species on the surface.

The following site balance is considered ($\Theta_{\text{B}} \approx 0$ due to rapid reversible desorption step and $\Theta_{\text{I2H}} \approx 0$, since the component is a short-living intermediate according to the pseudo-steady-state approximation).

$$\Theta_{\text{H}} + \Theta_{\text{I2}} + \sum \Theta_j + \Theta_{\text{V}} = 1 \quad (18)$$

The final rate expression for the heterogeneous step is obtained by inserting the adsorption equilibria (eqs 15–17) in the site balance (eq 18), solving the fraction of vacant

sites (Θ_V), and inserting the corresponding expression in the original rate equation (eq 14):

$$r_3 = \frac{k_3' c_{I_2} c_{H_2}}{(1 + K_{I_2} c_{I_2} + \sqrt{K_H c_{H_2}} + \sum K_j c_j)^3} \quad (19)$$

where $k_3' = k_3 K_{I_2} K_H$.

It is difficult to judge whether this is the absolutely correct mechanism for the heterogeneous hydrogenation step, because the step is relatively rapid compared to the homogeneous ones. Several competing mechanisms could be proposed, including, for example, a noncompetitive adsorption of the aromatics and the hydrogen molecules, which might approach the truth to some extent. It was impossible to prove whether the adsorption of hydrogen takes place dissociatively, as proposed here, or nondissociatively. Therefore the mechanism presented above should be considered more as an example of the modelling of a homogeneous–heterogeneous reaction system than as an absolutely correct mechanistic approach. For the same reason, the solvent effect on the catalyst surface did not play any decisive role, that is, the capability of the solvent to interact on the surface was not the main reason for choosing a suitable solvent.

On the basis of the reaction scheme and the stoichiometry, the generation rates for the reaction components are defined as follows, including both the catalytic and noncatalytic contributions, that is, $r_i = r_{i,\text{noncat}} + r_{i,\text{cat}} \rho_B c_M$:

$$r_A = -R_1 - R_9 \quad (20)$$

$$r_B = -R_5 - R_{10} + R_3 \rho_B c_M \quad (21)$$

$$r_C = -R_{11} + R_7 \rho_B c_M \quad (22)$$

$$r_D = -R_2 + R_{12} \rho_B c_M \quad (23)$$

$$r_E = -R_6 + (R_4 + R_{13}) \rho_B c_M \quad (24)$$

$$r_F = (R_8 + R_{14}) \rho_B c_M \quad (25)$$

$$r_{M2} = R_1 - R_3 \rho_B c_M \quad (26)$$

$$r_{M4} = R_5 - R_7 \rho_B c_M \quad (27)$$

$$r_{N2} = R_2 - R_4 \rho_B c_M \quad (28)$$

$$r_{N4} = R_6 - R_8 \rho_B c_M \quad (29)$$

$$r_{O2} = R_9 - R_{12} \rho_B c_M \quad (30)$$

$$r_{O4} = R_{10} - R_{13} \rho_B c_M \quad (31)$$

$$r_{O6} = R_{11} - R_{14} \rho_B c_M \quad (32)$$

To get a correct addition of the homogeneous and heterogeneous reaction rates, it is necessary to include the bulk density of the catalyst (ρ_B), and the concentration of the active metal on the catalyst (c_M , g of active metal/g of catalyst) for the heterogeneous steps.

Experimental Section

The experiments were carried out in a semibatchwise operating laboratory autoclave with a volume of 2000 mL. The autoclave was made of steel, and it was equipped with a turbine impeller and a temperature control system. The agitation speed was 1500 rpm. The aromatic reactant was dissolved in methanol, and the catalyst was placed in the

Table 1. Reaction conditions in nine reductive alkylation experiments^a

expt	t/min	T/°C	t _{feed} /min	c _{cat} /g mol ⁻¹	c _M /wt %	water (equiv)
1	300	50	240	3	5	0
2	300	60	240	3	5	0
3	270	75	240	3	5	0
4	330	30...40	240	3	5	0
5	570	30...40	300	3	3	0
6	300	75	240	3	5	3
7	300	50	240	3	5	3
8	330	30...40	240	3	3	0
9	360	30...40	60	2.5	3	2

^a p_{H₂} = 15 bar.

autoclave prior to the experiment, whereas the aldehyde and additional methanol as solvent were fed into the reactor during the experiment. Carbon-supported Pt with particle sizes of 6–70 μm (80%) was used as the catalyst. The amount of the catalyst was varied from 1 to 3 g of catalyst/mol of aromatic amine reagent, and the content of the active metal in the catalyst ranged from 3 to 5 wt %. Methanol was used as a solvent; at the end of the feed, the liquid phase contained about 70 wt % of methanol. The temperature interval of the experiments was 30–75 °C, and the hydrogen pressure was maintained at 15 bar. The experimental parameters are listed in Table 1. Samples were withdrawn from the reactor twice an hour, and the total reaction time varied between 4 and 10 h. The aromatic compounds were analyzed with high-performance liquid chromatography (HPLC), and for aldehydes and alcohols a gas chromatographic (GC) analysis was used.

Reactor Model and Mass Transfer in the Reactor

The laboratory scale reactor was operated semibatchwise as mentioned above. The reaction mixture was de facto a three-phase system, where the reactions proceeded in the liquid phase and on the surface of the solid catalyst. Since the catalyst particles were very small (Pt on activated carbon) and the agitation in the reactor was intensive, it was presumed that mass-transfer resistances at the outer surface of the catalyst and in the pores of the catalyst were negligible. Therefore a pseudohomogeneous model for the liquid–solid-phase reactions and for heterogeneously catalyzed reactions was assumed to be sufficient.

The generation rates as well as the gas–liquid interfacial fluxes and the reactant feeds are included in the liquid-phase mass balance, which obtains the following form:

$$dn_{Li}/dt = r_{i,\text{noncat}} V_L + r_{i,\text{cat}} \rho_B c_M V_L + N_{Li} a_V V_R + \dot{n}_{oi} \quad (33)$$

where i is the component index; ρ_B and c_M denote the catalyst bulk density ($\rho_B = m_{\text{cat}}/V_L$) and the concentration of the active metal on the catalyst, respectively. a_V gives the ratio of mass-transfer area to reactor volume ($a_V = A/V_R$).

When the liquid-phase concentrations are inserted into the mass balance, one obtains the equation

$$dc_{Li}/dt = (r_{i,\text{noncat}}V_L + r_{i,\text{cat}}\rho_B c_M V_L + N_{Li}a_V V_R + (c_{0i} - c_{Li})\dot{V}_0)/V_L \quad (34)$$

by assuming that the liquid-phase volume change is caused exclusively by the reactant feed, that is, $dV_L/dt = \dot{V}_0$.

After introducing the space time ($\tau = V_L/\dot{V}_0$), the balance takes the form

$$dc_{Li}/dt = r_{i,\text{noncat}} + r_{i,\text{cat}}\rho_B c_M + \frac{N_{Li}a_V}{\epsilon_L} + \frac{c_{0i} - c_{Li}}{\tau} \quad (35)$$

where $\epsilon_L = V_L/V_R$ is the liquid-phase holdup. The generation rates in eqs 20–32 are defined as $r_i = r_{i,\text{noncat}} + r_{i,\text{cat}}\rho_B c_M$. Since the flow into the liquid phase is assumed to be constant, the liquid volume is obtained by the trivial integration of the reactant feed with respect to feed time. The changes of τ and ρ_B are obtained analogously.

Hydrogen was fed into the autoclave, and the total pressure was maintained constant. Principally, the gas-phase mass balance of an arbitrary component is written as follows:

$$dn_{Gi}/dt = -N_{Gi}A + \dot{n}_{G0i} \quad (36)$$

Since it is reasonable to assume that hydrogen is the dominant compound in the gas phase, the balance is written exclusively for hydrogen:

$$dn_{G,H_2}/dt = -c_{H_2}\dot{V}_0 \quad (37)$$

which is easily expressed with the concentration:

$$dc_{G,H_2}/dt = 0 \quad (38)$$

In practise, the hydrogen concentration in the gas phase is calculated from an equation of state. The validity of the assumption that hydrogen dominates in the gas phase was tested by calculating the solvent (methanol) vapour pressure: if the vapour pressure of methanol at the reaction temperature is considerably lower than the reactor pressure, it can be concluded that the assumption is valid, since the vapour pressures of the aromatics are quite low and aldehyde concentration in the reactor is usually very low. The vapour pressure of methanol ($p_{\text{MeOH}}^{\text{vap}}$) is calculated from the Antoine equation and applying Raoult's law:

$$p_{\text{MeOH}}^{\text{vap}}/\text{bar} = x_{\text{MeOH}} \left(A_{\text{MeOH}} - \frac{B_{\text{MeOH}}}{T/K + C_{\text{MeOH}}} \right) \quad (39)$$

The parameters A , B , and C for methanol were extracted from the databank of Reid et al.:⁵ $A = -8.547\,96$, $B = 0.769\,82$, and $C = -3.108\,50$. The flux of hydrogen from the gas phase into the liquid phase was assumed to obey the Fickian law for nonreactive gas and liquid films,

$$N_{GH_2} = N_{LH_2} = \frac{c_{GH_2} - K'_{H_2}c_{LH_2}}{\frac{K'_{H_2}}{k_{LH_2}} + \frac{1}{k_{GH_2}}} \quad (40)$$

where K_{H_2} denotes the gas–liquid equilibrium ratio of hydrogen and k_{GH_2} and k_{LH_2} are the mass-transfer coefficients for the gas and liquid films, respectively. The denominator of eq 40 can be lumped to a single parameter,

$$\frac{1}{k'_{H_2}} = \frac{K'_{H_2}}{k_{LH_2}} + \frac{1}{k_{GH_2}} \quad (41)$$

where k'_{H_2} is an abbreviation for the overall mass-transfer coefficient.

After introducing the ratio a_V we obtain

$$N_{H_2}a_V = k'_{H_2}a_V(c_{GH_2} - K'_{H_2}c_{LH_2}) \quad (42)$$

The gas–liquid equilibrium ratio for hydrogen (K'_{H_2}) in eqs 40–42 is defined accordingly:

$$K'_{H_2} = c_{GH_2}/c_{LH_2} \quad (43)$$

which is related to the thermodynamic equilibrium ratio K_{H_2} , in the following way:

$$K'_{H_2} = K_{H_2}c_G/c_L \quad (44)$$

where c_G and c_L are the total concentrations of gas and liquid, respectively. The total concentration of the liquid phase is calculated approximately in the following way: $c_L \approx \sum c_{Li}$. The total concentration in the gas phase is obtained from the equation of state.

Henry's law and a hydrogen solubility correlation were applied for the calculation of hydrogen mole fraction in the liquid phase (x_{H_2}) and K'_{H_2} , and exclusively hydrogen was assumed to exist in the gas phase. According to Henry's law,

$$He'_i = p_i^s/x_{Li}^s \quad (45)$$

Henry's constant He'_i is defined by the partial pressure of the gas (p_i^s) and the mole fraction of the dissolved gas in the liquid phase (x_{Li}^s). For the calculation of hydrogen solubility at $p_i^s = 1.013$ bar, the equation given by Fogg and Gerrard⁶ was used:

$$\ln x_{Li}^s = -7.3644 - 408.38/(T/K) \quad (46)$$

It is reasonable to assume that the hydrogen solubility in the reaction mixture is close to the solubility of hydrogen in methanol, because the methanol concentration always exceeded 50 wt %.

If the vapour pressures of the compounds in the liquid phase are so high that considerable amounts of these compounds escape into the gas phase, more rigorous calculations of the vapour–liquid equilibria should be applied. Cubic equations of state can be used for the calculation of the fugacity coefficients and the vapour–liquid equilibria,

(5) Reid, R. C.; Prausnitz, J. M.; Poling, B. E. *The Properties of Gases and Liquids*, 4th ed.; McGraw-Hill, Singapore, 1988.

(6) Fogg, P. G. T.; Gerrard, W. *Solubility of Gases in Liquids*; J. Wiley & Sons: Chichester, 1991; p 300–303.

or an appropriate activity coefficient model can be applied for the calculation of the liquid-phase activities.

Parameter Estimation Procedure and Estimation Results

The kinetic model and the laboratory scale reactor model were implemented in the software MODEST⁷ for the estimation of the rate parameters. The ordinary differential equation (ODE) system was solved with the backward difference method⁸ for stiff (ODE) systems implemented in the LSODE software,⁹ and the objective function was minimized using the Levenberg–Marquardt method.¹⁰ The concentrations of the aromatic reactant (**A**), the monoalkylated product (**B**), and the dialkylated product (**C**) were included in the objective function (Q) accordingly,

$$Q = \sum_j [(c_{A_j} - \hat{c}_{A_j})^2 + (c_{B_j} - \hat{c}_{B_j})^2 + (c_{C_j} - \hat{c}_{C_j})^2] \quad (47)$$

where \hat{c}_{ij} denotes a concentration predicted by the model at the reaction time “ t ”. The concentrations of the ring-alkylated components (**D–F**) were so low that they were discarded from the objective function. A total of nine experiments were considered in the parameter estimation. The experimental conditions are listed in Table 1. The abbreviations in Table 1 are explained in Notation.

The experiments were merged together into a single set, and the parameters were estimated simultaneously. The solubility of hydrogen in the liquid phase was calculated according to eqs 55 and 56. The overall mass-transfer coefficient of hydrogen was assumed to be at a high level (de facto no mass-transfer resistance). The methanol vapour pressure was estimated using Antoine’s equation and Raoult’s law (eq 46). The values of the kinetic and the adsorption equilibrium parameters are given in Table 2a. As can be seen from Table 2a, the degree of explanation (R^2 value) is quite high, but the identifiabilities of the rate and adsorption equilibrium parameters of the heterogeneous step were poor.

Since reactions 3 and 7 were observed to have some important rapid steps, high values were given to the rate constants and the adsorption equilibrium parameters were presumed to be nil. The remaining parameters were re-estimated, and values are given in Table 2b. Although this four-parameter system gives almost the same R^2 value, Table 2b also reveals that the significance of the activation energies is very low. Therefore the parameter estimation was repeated again including just the reaction rates of reactions 1 and 5. The estimated parameter values are presented in Table 2c. The R^2 value decreased from 97.4% to 96.8%, but still, it is very reasonable to describe the actual reaction system with two parameters only. The fits of the model with four parameters and with two parameters are compared in Figure 1.

Table 2

(a) Kinetic and Adsorption Parameters					
$R^2 = 97.66$	$A/\text{dm}^3 \text{ mol}^{-1} \text{ min}^{-1}$	$\sigma/\%$	$E_a/\text{J mol}^{-1}$	$\sigma/\%$	
k_1	0.119	9.3	87.3	215	
k_5	0.0306	10.7	22 690	11.0	
<hr/>					
	$A/(\text{dm}^3)^2 (\text{g of active metal})^{-1} \text{ mol}^{-1} \text{ min}^{-1}$	$\sigma/\%$	$E_a/\text{J mol}^{-1}$	$\sigma/\%$	
k_3	85.43	109	488.2	214	
k_7	5.4×10^{16}	0.0	651 700	181	
<hr/>					
	$K_{\text{ADS}}/\text{dm}^3 \text{ mol}^{-1}$			$\sigma/\%$	
K_{AR}	2.54×10^{-10}			157	
$K_{\text{H}_2\text{O}}$	5.49×10^{-04}			183	
K_{H_2}	1.21×10^{-03}			259	
K_{MeOH}	4.34×10^{-03}			194	
<hr/>					
(b) Kinetic Parameters with Four-Parameter Simplification					
$R^2 = 97.63$	$A/\text{dm}^3 \text{ mol}^{-1} \text{ min}^{-1}$	$\sigma/\%$	$E_a/\text{J mol}^{-1}$	$\sigma/\%$	
k_1	0.120	8.6	20.5	1230	
k_5	0.0313	9.3	23 200	9.4	
<hr/>					
(c) Kinetic Parameters with Two-Parameter Simplification					
$R^2 = 96.76$	$k/\text{dm}^3 \text{ mol}^{-1} \text{ min}^{-1}$		$\sigma/\%$		
k_1	0.073		7.3		
k_5	0.013		7.3		

The estimation of the overall mass-transfer coefficient for hydrogen was also tested. It was noticed that the gas–liquid mass-transfer resistance of the hydrogen was not the rate-limiting step in the heterogeneous reactions and that the activation energies of the homogeneous step cannot be attributed to the mass-transfer limitation. On the other hand, the solubility of hydrogen in the liquid phase probably limits the rates of heterogeneous reaction steps and can also have an influence on the activation energies of the homogeneous step. Anyway, it can be concluded that the estimated rate parameters describe very truly the velocities of the homogeneous steps.

Conclusions

A reaction scheme for reductive alkylation of aromatic amines was proposed including reductive monoalkylation and dialkylation reactions of the amino group as well as reductive alkylation of the aromatic ring (Scheme 1). These three types of reactions involved both homogeneous and heterogeneous reaction steps. Kinetic equations were derived starting from probable chemical mechanisms, and the kinetic model was combined with a reactor model for a three-phase semibatch reactor. The kinetic parameters were estimated for the model reaction system (reductive alkylation), and it was concluded that the number of adjustable parameters in the model could be considerably reduced without any decisive deterioration of the fit of the model (Table 2a–c and Figure 1) on the laboratory scale. However, there is no evidence for how scale-up of the reactions to the industrial scale affects the

(7) Haario, H. *MODEST-User's Guide*; Profmath Oy: Helsinki, 1994.
 (8) Henrici, P. *Discrete Variable Methods in Ordinary Differential Equations*; Wiley: New York, 1962.
 (9) Hindmarsh, A. C. A Systematized Collection of ODE-Solvers. In *Scientific computing*; Stepleman, R., et al., Eds.; IMACS/North Holland: Amsterdam, 1983; pp 55–64.
 (10) Marquardt, D. W. An Algorithm for Least Squares Estimation on Nonlinear Parameters. *SIAM J.* **1963**, 431–441.

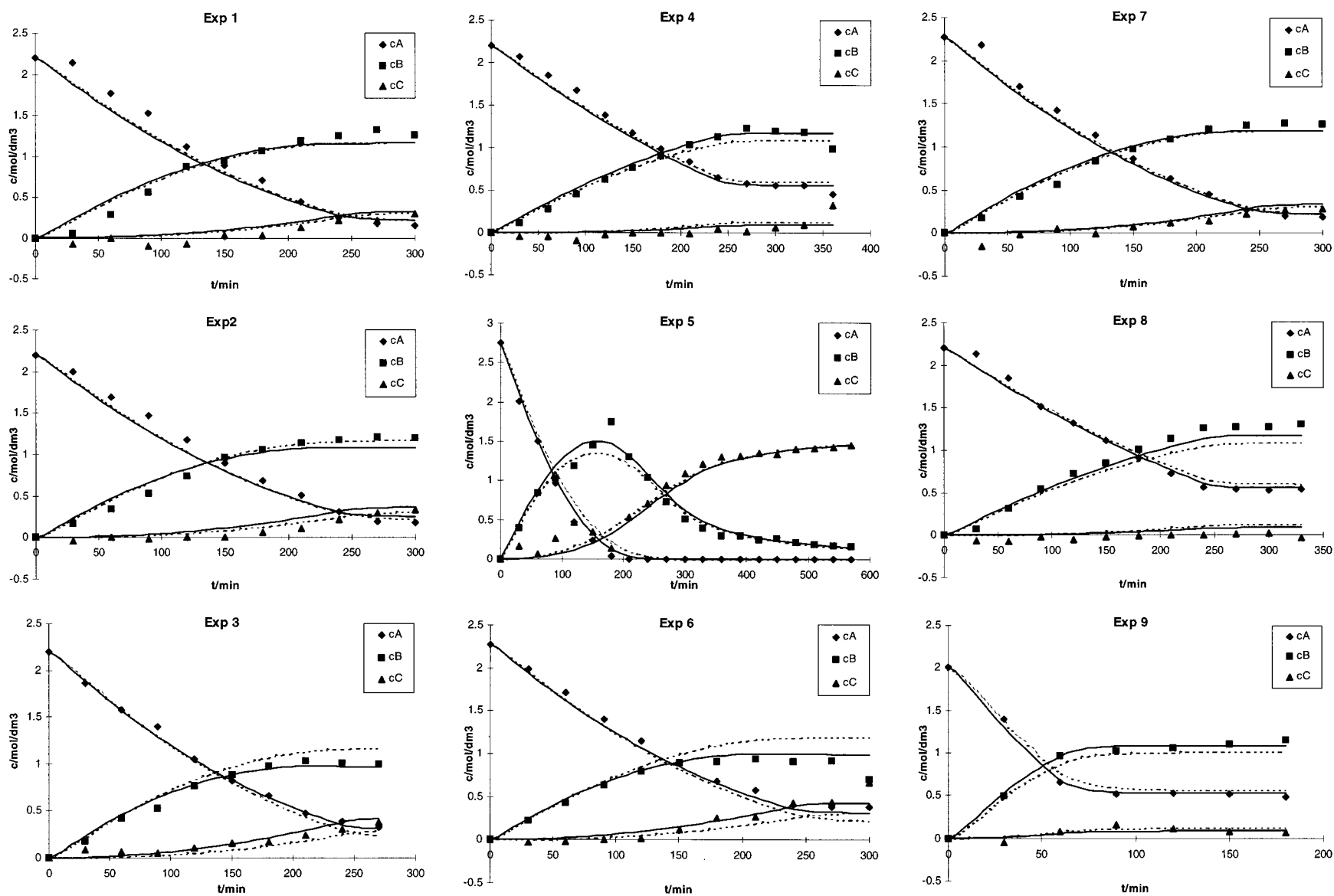


Figure 1. Fits of the model of nine experiments. The solid lines give the model prediction with four parameters, and the dotted lines give the model prediction with two parameters; cA, cB, and cC denote concentrations of components A, B, and C, respectively.

system and how the intrinsic kinetics can be applied to a reactor with remarkable mass-transfer limitations. These expected problems in the scale-up will be discussed later by our group.

NOTATION

A	gas-liquid interfacial area
a_V	ratio of gas-liquid interfacial area to reactor volume
c	concentration
K	equilibrium constant; adsorption equilibrium parameter
K'	vapour-liquid phase-equilibrium constant
k	rate constant
k_G	mass-transfer coefficient in the gas film
k_L	mass-transfer coefficient in the liquid film
m	mass
N	flux
n	amount of substance
\dot{n}	molar flow
p	pressure
p^s	saturation pressure
p^{vap}	vapour pressure
Q	objective function
R	gas constant
R	reaction rate
r	generation rate
T	temperature
t	time
V	volume
V_L	liquid-phase volume
V_R	reactor volume
\dot{V}_0	feed flow of liquid
x	liquid-phase mole fraction
y	gas-phase mole fraction

Z	compressibility factor
ϵ_L	holdup
ϕ	fugacity coefficient
ρ_B	catalyst bulk density
Θ	site fraction
τ	space time

Subscript and Superscripts

cat	catalyst, catalytic contribution
G	gas phase
i	component index
j	reaction index
L	liquid phase
M	active metal
noncat	noncatalytic contribution
R	reactor
s	saturation
0	feed
\wedge	a property predicted by the kinetic model
*	active surface site on the catalyst

Abbreviations

A-F	reaction components
H	hydrogen
I1	intermediate 1
I2	intermediate 2
M1-M4, N1-N4, O1-O6	reaction components (intermediates)
R'CHO	aldehyde

Received for review June 26, 1997.

OP970032F